

# ALKALI SILICA REACTION IN CONCRETE FOUNDATIONS IN THAILAND

Viggo Jensen <sup>1\*</sup>, and Suvimol Sujjavanich <sup>2</sup>

<sup>1</sup>Norwegian Concrete and Aggregate Laboratory LTD, Sorgenfrivein 11, 7031 Trondheim, NORWAY

<sup>2</sup>Kasetsart University, Faculty of Engineering, Department of Civil Engineering, 50 Paholyothin Rd. Chatuchak, Bangkok 10900, THAILAND

## Abstract

The paper demonstrates the occurrence of deleterious Alkali Silica Reaction (ASR) in mass concrete foundations from a superstructure of motorways bridges located in Thailand. ASR is caused by slow reactive sericite rock, quartzite and granite with and without cataclastic texture. Signs of reactions are similar to reaction of slow-reactive aggregates reported in literature. Microstructural analyses on fluorescence impregnated polished slabs and thin sections show that ASR occurs simultaneously with delayed ettringite formation (DEF). Damage is moderate according to Norwegian experience. Thai cements are low alkali and should therefore not be susceptible to ASR for slow-reactive aggregates. In a separate paper, the authors present analyses on reaction products from the same concretes and discuss the possibility that high initial temperature and DEF might have activated slow-reactive aggregates to be alkali reactive.

**Keywords:** Concrete, Alkali Silica Reaction (ASR), Delayed Ettringite Formation (DEF), Petrography, Scanning Electron Microscopy/Energy Dispersive X-ray spectrometry (SEM/ EDX)

## 1 INTRODUCTION

Analyses of concrete core samples from mass concrete foundations confirm the first case of Alkali Silica Reaction (ASR) in Thailand. The investigated concrete foundations are parts of an approximately 50 km long highway infrastructure in the central part of Thailand near Bangkok. The Highway was open for public use in 1998 before completion.

The construction project involved multiple subcontractors and different sources of materials. The precast-and prestressed box girder bridge structure is supported by huge mass concrete foundations with dimensions approximately 5 m x 11 m x 2.5 m. Cracks in the foundations were observed a short time after the construction period and were partially repaired with epoxy. Later inspections revealed that the repaired cracks still were expanding and new cracks had formed (see Figure 1). An initial condition assessment in 2005 reported extensive map cracking in about 20 % of the surveyed foundations, and that damage varied from one foundation to another, from none to severe [1]. A field inspection by the authors in 2013 revealed beginning map cracking and long vertical up to 0.5 mm wide cracks in some of the pillars on the box girder structure.

Petrographic analyses and Uranyl Acetate tests on cored samples taken after 10 years of service suggested occurrence of ASR caused by reaction of fine grain black quartzite and granite [1], [2]. Ettringite occurred in small air voids and in elongated air voids and it was first anticipated as one of the potential causes of expansion from the high temperature in mass concrete. However, it was later assessed that ettringite not was the cause of internal expansion or micro cracking in the concrete [3].

Study on other foundations performed by other research groups observed combined occurrence of delayed ettringite formation (DEF) and ASR [4]. It was concluded that DEF and ASR are the two main causes of cracks in the foundations [4]. Simulation tests of semi-adiabatic temperature rise in mass concrete showed temperature over 70°C, suggesting the condition for DEF was present in the concrete [4]. Other expansion tests on cored concrete samples showed varying expansion results, indicating some of the foundations could be susceptible for ASR [1], [2].

---

\* Correspondence to: [viggo.jensen@nbt.no](mailto:viggo.jensen@nbt.no)

This investigation is based on two concrete cores marked “sample 30-XA” (concrete core Ø 75 mm and length 100 mm) and “sample 30-XB” (concrete core Ø 75 mm x 205 mm) taken from two different mass concrete foundations showing intense cracking in 2008/2009. The cores are part of an extensive research program where 10 concrete foundations have been cored [1]. From each sample, one fluorescence impregnated polished slab (sawed parallel with the length axis of the core sample), two normal size fluorescence impregnated thin sections and one polished thin section for SEM/EDX analysis, have been prepared. The polished slabs and thin sections in both samples are located in the centre of the cores. The cores are examined by micro-structural analysis and SEM/EDX analysis and the findings are reported and discussed in the paper. Detailed analyses of reaction products and DEF are presented in a separate paper by the authors [5].

It has not been possible to obtain information on the concrete composition (e.g., type of cement and aggregates used in the concrete). However, it is most likely local Thai cement and aggregates from a local deposit near the construction sites were used for concreting. Laboratory investigation of samples from some commercial aggregate quarries in the same area near the construction sites showed aggregates to be potential reactive [6].

## 2 THAI CEMENTS

Due to normal practice in Thailand, local Thai Cements are used for concreting the foundations. Imported cements are normally not in use in Thailand and were likely not used during the construction period.

Table 1 gives chemical composition of Thai cements from literature in the period 2000-2012 [7], [8], [9], [10], [11], [12], [13], [14]. Note that all cements have low alkali content with eq. Na<sub>2</sub>O (eq. Na<sub>2</sub>O = Na<sub>2</sub>O + 0.658 K<sub>2</sub>O) varying from 0.20 to 0.48, which classifies all the cements to be low alkali cements (< 0.6 % eq. Na<sub>2</sub>O-eq.). The alkali content of cement is very important for the susceptibility for ASR in concrete.

## 3 GEOLOGY AND AGGREGATES

According to the local geological map the following aggregates types are located near the construction sites [15].

- Alluvial deposit, beach sand
- High and low terrace deposit, laterite, gravel, sand, silt and clay
- Bedrock of yellow-brown quartzite, quartz, schist, grey slate, shale, black slate, quartzitic sandstone interbedded with dark grey argillaceous limestone with fossils of Nautilus
- Bedrock of medium-grained leucocratic-mesocratic colour, locally porphyritic biotite muscovite granite, pegmatite veins and quartz dikes.
- Bedrock of quartz-mica schist and quartz-kyanite schist

Note that volcanic rocks are not present in the area.

Observations from investigated concretes suggest that the fine fractions (sand) used in the concretes most likely are from local terrace deposits of gravel and sand or river sand. The coarse aggregates in the concrete, which are crushed sericite rock, quartzite and granite rock (and lesser limestone), most likely originate from local quarries that produce crushed rock in the area to local construction sites.

In the following, descriptions of aggregates that have reacted in the concretes are given.

## 4 PETROGRAPHIC DESCRIPTION OF AGGREGATES REACTED IN CONCRETES

### 4.1 Sericite rock

Sericite rock is the dominant crushed coarse aggregate in sample 30-XA. The sericite rock is dense, dark grey to light grey (greenish), dominated by anhedral sericite (microcrystalline mica) and lesser feldspar, biotite, carbonate, chlorite and opaque phases. Thin veins and “larger areas” of microcrystalline quartz occur in the rock. Crystal sizes of the sericite are up to 0.01 mm, and up to 0.2 mm for quartz. Micro texture varies between particles and can be structure less, slightly laminated or spotted. Some particles appear with flow structures. Lens-formed pseudo morphs of relict minerals up to 1 mm and relict textures can be observed in several particles. The rock is probably altered (sericitized) feldspar-containing rock of unknown origin. Semi-quantitative EDX analyses are given in Table 2.

### 4.2 Granite

Granite has been used as coarse crushed aggregate in sample 30-XB. The granite particles, which are medium grained, contain strained quartz-feldspar, muscovite and both unaltered areas and altered areas by

cataclase (dynamically metamorphosed). Some particles or areas in particles could be classified as cataclasite. Some granite particles have porphyroclastic texture. Porphyroclasts (or porphyroblasts in cases of cataclase) consist of feldspar and intergrown feldspar - quartz surrounded by a finer matrix of quartz, feldspar, mica and opaque phases. Quartz veins are observed in several particles.

#### **4.3 Quartzite**

Quartzite comprises the coarse crushed aggregate in sample 30-XB. The quartzite is dark grey, dense and structureless, dominated by intergrown anhedral quartz and less sericite, epidote, chlorite and varying content of opaque phases. Crystal sizes are 0.05-0.01 mm. Some particles have relict structures (with sericite) and high content of up to 1 mm euhedral opaque phases. The rock is of unknown origin. Semi-quantitative EDX analysis is given in Table 3.

### **5 MICROSTRUCTURAL ANALYSIS**

#### **5.1 Introduction**

Microstructural analysis is an examination method of hardened concrete with use of different visual techniques including microscopic examination of polished fluorescence-impregnated polished slabs (PS) and thin sections (TS). Microstructural analysis is suitable for assessment of concrete quality; concrete composition, materials, damage and deterioration processes, and is especially useful for examination of Alkali Silica Reaction in concrete [16]. For “sample 30-XA” and “sample 30-XB”, the first step of the examination was a visual examination of signs of ASR in the core, e.g. observations of cracking and reaction products. The polished fluorescent-impregnated slabs (PF) were examined under stereomicroscope in ordinary light and UV light. Thin sections (TS) were examined under the polarizing microscope, which was mounted with UV filters. Polished thin sections (PTS) from each sample were examined by petrographic microscope in addition to SEM/EDX examinations.

#### **5.2 Composition of the concretes**

The coarse aggregates in sample 30-XA are dominated by crushed dark grey dense to fine grained sericite rock with maximum cross-sections of about 20 mm. In sample 30-XB, the coarse aggregates consist of crushed granite, crushed dark grey dense-fine grained quartzite and few particles of crushed white carbonate rock, with maximum cross-sections of about 13 mm. In both samples, the fine aggregate (sand) is of natural origin, consisting of quartz, quartzite, feldspar and various rock fragments. Quartz is sometimes highly strained. In both concretes, the cement paste is proportioned from Portland cement without signs of supplementary additions and with “normal” hydrations and distribution of portlandite. The air void content is less than 3 % - 4 %, with a few air voids up to 2-8 mm.

#### **5.3 Signs of reaction, reaction products and ettringite**

ASR is observed in coarse crushed aggregates of sericite rock, quartzite and granite with cataclastic texture. In sample 30-XA, the presence of reaction rims on the broken face, white reaction products in air voids and white reaction products in aggregates on sawn faces suggest the occurrence of ASR. In sample 30-XB, the surface contains white reaction products in dark grey dense quartzite and on some granite particles, also suggesting ASR. Figure 2 shows white reaction products in reacted quartzite and micro-cracks due to ASR as seen in UV-light. Two types of ASR reaction products can be observed in thin sections, namely, cryptocrystalline reaction products in reacted aggregates and amorphous gel (sometimes laminated and recrystallized). Gel occurs in peripheral micro-cracks in the contact zone of the cement paste and the aggregate (some intergranular), and fewer in micro-cracks in the cement paste. Alkali gel has not been observed in air voids in thin sections but in core material. In reacted aggregates, cryptocrystalline reaction products in cracks are succeeded by amorphous gel in the contact zone with the cement paste as normally observed in slow reactive aggregates. In some sericite rock, intergranular cracks oriented near and along the interface are filled with gel. In sericite rock and quartzite, the amount of ASR reaction products and micro cracking is significant. In reacted granitic particles, the amount of ASR reaction products is insignificant while cracking is significant.

A significant amount of fibre, needles and fan-shaped agglomerates of ettringite is precipitated in micro-cracks in the cement paste, more or less filling air voids. Peripheral micro-cracks surrounding coarser aggregates are more or less filled with ettringite.

Figure 3 show reaction signs and reaction products from reacted sericite rock (sample 30-XA). Figure 4 shows reaction signs and reaction products from reacted granite and quartzite (sample 30-XB). Figure 4 B shows inter granular micro cracking and dense outer rim in reacted granite under fluorescence light.

#### 5.4 Micro-cracks

Micro-cracks appear in reacted aggregates (intergranular) and in several cases also extend into the cement paste, suggesting deleterious ASR. Micro-cracks are maximum 0.1-0.2 mm wide in thin sections. In fluorescence light some reacted particles contain a high content of intergranular micro-cracks and a dense outer zone as sometimes observed in reacted slow reactive aggregates. Micro-cracks, which extend into the cement paste and connect other reacted particles, suggest that deleterious ASR is at an advanced stage. Micro-cracks in the cement paste are abundant and several coarser aggregates (and some finer) are surrounded by peripheral micro-cracks filled with ettringite. Peripheral micro-cracks are more pronounced in sample 30-XA and less in sample 30-XB.

Figure 2 shows micrographs of cracks on polished fluorescence impregnated polished slabs photographed in UV light.

#### 5.5 Damage rate, Norwegian method

Determination of cracking and damage has been carried out according to Norwegian procedures [16], [17]. It is important that examination by use of thin section first has been carried out for documentation for potential ASR. First the fluorescence-impregnated polished slabs are examined under normal light and number of particles  $> 4$  mm is counted and the dimensions of the slab are measured. Hereafter, and under UV light the number of particles with cracks, number of particles where cracks runs out in the cement paste and number of cracks in the cement paste are counted. The percentage of particles with cracks and percentage of particles with cracks extending into the cement paste are calculated and the number of cracks in cement paste normalized to number of cracks/cm<sup>2</sup>.

The results from counting Thai concretes in addition to a calculated crack index is given in Table 4 [17], [18]. Note that ASR is assessed deleterious reaction types 5 where cracks due to ASR extends into the cement paste and connects reacted particles [16]. The Norwegian crack index classifies Thai concretes to be “moderate to severe ASR” (samples 30-XA) and “small to moderate ASR” (sample 30-XB), or generally as “moderate ASR”. A graphical plot of the number of cracks in the cement paste versus the percentage of coarse particles with cracks is plotted together with Norwegian structures damaged by ASR [16], including results from the NBTL laboratory over several years, see Figure 5. Note that sample 30-XA and 30-XB from Thailand plots in the same “cluster” as Norwegian structures damaged by deleterious ASR.

## 6 SUMMARY AND DISCUSSION

### 6.1 Cracking in concrete foundations

Intense mesh-like cracking in the concrete foundations was observed a few years after the construction (1998) and many foundations were repaired with epoxy. Later inspections showed that repaired cracks were still expanding and new cracks had developed, suggesting an ongoing damaging process. In addition to the mesh-like cracking, many concrete foundations contain both horizontal and vertical cracks, some measured to be 9 mm wide (see Figure 1). Field inspection in 2013 by the authors revealed beginning map cracking and fine vertical cracks in some of the box girder pillars suggesting the initiation of ASR. Microstructural analyses show occurrence of deleterious ASR caused by slow-reactive aggregates and simultaneous DEF in form of peripheral micro-cracks surrounding aggregates (gap-grading) and high amounts of ettringite in cracks. The mesh-like cracking pattern observed in foundations most likely is caused by DEF or ASR, or a combination of both mechanisms. Because ASR is due to slow-reactive aggregates, it is very likely that early cracking is caused by DEF and ongoing later cracking by ASR. In the superhighway structure, only a few concrete foundations are exposed above ground level. Most of the concrete foundations are buried below ground level and are thus not possible to inspect. The condition of buried foundations is unknown. In a separate paper the authors present and discuss the sequential appearance of ASR and DEF and the possibility that DEF might have activated slow-late reactive aggregates to be alkali reactive [5].

### 6.2 Cement

Thai cements have low alkali content with eq. Na<sub>2</sub>O varying from 0.20 to 0.48. The “survey” EDX analyses in Table 4 also suggest the use of low alkali cement in the concrete. At the present time when information on the cement not is available, one has to presume that local Thai low alkali cement was used for concreting. Today there are no reliable methods for assessment of alkalis available for ASR or the alkali content in the cement in hardened concrete. According to literature, low alkali cement should not be susceptible to causing ASR for slow expansive aggregates [19], [20]. Therefore, it would have been expected that ASR should not have developed due to reaction from slow-reactive aggregates in the concrete. It is possible that high temperature during the construction period (hardening of the concrete) has influenced the development of ASR.

### 6.3 Reactive aggregates

Deleterious ASR is documented by use of microstructural analyses in two concrete foundations. ASR is caused by reaction of crushed coarse aggregate composed of sericite rock, quartzite and granite with and without cataclastic texture. The origin of these aggregates is unknown but similar types are reported in local geological mapping. Quartzite and granite are both rock types reported to be alkali reactive in literature. Granite is partly altered by cataclase (dynamically metamorphosed) and part of the particle could be named “cataclasite”, which can have increased the reactivity of the granite.

Sericite rock has not formerly been reported as potentially alkali reactive in concrete [19]. Sericite rock is most likely of sedimentary origin because volcanic rocks are not reported in the local geological map. The reactivity of sericite rock is probably increased due to the sericitization process, which transforms feldspar into sericite (fine grained muscovite) and secondary silica as microcrystalline quartz [21]. Microcrystalline quartz is well known to be alkali reactive and is observed in most of the sericite rock particles.

### 6.4 Signs of reaction, micro-cracks and quantification of damage

Signs of reaction in sericite rock, quartzite and granite are similar to reaction of slow-reactive aggregates reported in literature. Occurrence of cryptocrystalline reaction products and internal cracking in aggregates, as well as amorphous alkali gel in the cement paste, is characteristic.

In ordinary and fluorescent light, micro-cracking is distinct in reacted aggregate. Cracks from aggregates that extend into the cement paste suggest deleterious ASR [16]. In some aggregate, a “dense” outer zone can be observed in fluorescent light, which often is seen in reaction of slow reactive aggregates [16].

Quantification of micro-cracks by the “Norwegian method” plots the Thai concretes into the same “cluster of damage” as many Norwegian structures. The Norwegian crack index classifies Thai concretes to be “moderate ASR”. Thai cores are smaller than normally examined in Norway and therefore less representative. However, the result gives a more or less correct estimate of the damages in the concretes.

## 7 CONCLUSION

Microstructural analyses confirms that deleterious ASR has damaged and cracked the Thai concrete foundations. ASR is caused by reaction from coarse slow-reactive sericite rock in concrete foundation sample 30-XA and coarse slow-reactive quartzite and granite with and without cataclastic texture in concrete foundation sample 30-XB. The signs of reaction are morphologically similar to those observed by reaction from slow-reactive aggregates reacted in Norway and universally. Damages can be classified as “moderate ASR” according to Norwegian experiences. Thai cements are all with low alkali content and therefore not susceptible to ASR from slow-reactive aggregates. In a separate paper, the authors present results of SEM/EDX analyses and characteristics of reaction products, and discuss the possibility that DEF might have activated slow-reactive aggregates to be reactive and therefore “trigger” ASR [5].

## 8 REFERENCES

- [1] S. Sujjavanish, P. Suwanvitaya, D. Rotstein, Investigation of ASR in Mass Concrete Structures: a Case Study, in S. O. Cheung, N. Ghafoori and A. Singh (eds), Modern Methods and Advances in Structural Engineering and Construction, ISEC-6, Zurich, June 21-26, 2011.
- [2] D. Rothstein, Technical report of Petrographic Investigation of a Concrete Extracted from a Bridge Pier Toll Way located in Bangkok, Thailand, report no.: DRP09.587 prepared for Department of Civil Engineering Kasetsart University, Feb. 2009.
- [3] Kasetsart University, Civil Engineering Department 2009, Extended Report on Continued Deterioration Assessment on Expansion of Mass Concrete. Interim Report, Kasetsart University for the Expressway Authority of Thailand C.E. Department (in Thai).
- [4] L. Baingam, W. Saengsoy, P., P. Choktaweekarn, S. Tangtermsirikul, Diagnosis of a combined Alkali Silica reaction and Delayed Ettringite Formation, Thammasat International Journal of Science and technology, vol. 17, no.4, October-December 2012.
- [5] V. Jensen and S. Sujjavanish : ASR and DEF in Concrete Foundations in Thailand, Proc. 15<sup>th</sup> Int. Conf. ASR, Sao Paulo, Brazil, 2016.
- [6] Sujjavanich S., et al. 2012, Investigation of potential alkali-silica reactivity of aggregate sources in the eastern part of Thailand (in Thai). the 8th Annual Concrete Conference, Chonburi Thailand, 2012.
- [7] S. Sayamipak , Development of Durable Mortar and Concrete Incorporating Metakaolin from Thailand, Asian Institute of Technology. Ph.D. Thesis, Thailand, 2000.
- [8] S. Sujjavanich, P. Suwanvitaya, M. Sarikabhuti, Effect of Accelerated Curing Conditions on Microstructure and Strength of Fly Ash and Strength of Fly Ash Cement Mortar, the 4th Regional Symposium on Infrastructure Development in Civil Engineering (RSID4), Bangkok, Thailand, 2003.

- [9] M. Teekavanit et.al, Effects of Sea Water on Chloride Penetration and Corrosion of Reinforcing Steel in Fly Ash Concrete, the 10th NCCE, Pattaya, 2002 (in Thai).
- [10] J. Suwanapruk, S. Sujjavanich, Impact of Low Sulfate Metakaolin on compressive Strength and Chloride Resistance of High Strength Concrete, the 4th Regional Symposium on Infrastructure Development in Civil Engineering (RSID4), Bangkok, Thailand, 2003.
- [11] S. Sa-ardkitinun et al., A modified ACI Mix design method for high strength concrete with classified and unclassified Mae Moh fly ash, the 9th NCCE, Khon Kean, Thailand 2004 (in Thai).
- [12] B. Chatveera and N. Makul, effect of very fine ground white RHA on Mechanical properties of concrete, the 9th NCCE, Khon Kean, Thailand, 2004 (in Thai).
- [13] Report of PFA and Cement Analysis, Innovation and Technology Division, CPAC Co.Ltd., Thailand, 2010.
- [14] G. Sua-Iam and N. Makul, The Microwave Curing Effects on Strength Development of Flowable Concrete, the 8th ACC, UbonRatchathani Thailand, 2008 (in Thai).
- [15] Geological map of Thailand 1 : 250000, Bangkok Metropolis, published by Geological Survey Division Department of Mineral Resources, 1984.
- [16] V. Jensen, Alkali Aggregate Reaction in Southern Norway, Doctor Technicae Thesis, The Norwegian Institute of Technology, Trondheim, Norway, 2003, pp 262.
- [17] J. Lindgård, B. Wigum, Alkali Aggregate Reaction in Concrete - Field Experiences, SINTEF report, STF22 A02616, Trondheim, 2003 (in Norwegian).
- [18] J. Lindgård et.al, Experienc from evaluation of degree of damage in fluorescent impregnated plan polished sections of half-cores based on the crack index method, 12th ICASR, 2004.
- [19] V. Jensen, Reclassification of Alkali Aggregate Reaction”, in Proc. 14<sup>th</sup> Int. Conf. ASR, T. Drimalas, J. H. Idekar, B. Fournier (eds), Austin, Texas, USA, 2012, p 12.
- [20] RILEM State-of-the-Art Reports, Guide to Diagnosis and Appraisal of ASR Damage to Concrete in Structures, Part 1 Diagnosis (ASR 6.1), Volume 12 2013, Editors: Bruno Godart, Mario de Rooij, Jonathan G.M. Wood, ISBN: 978-94-007-6566-5 (Print) 978-94-007-6567-2 (Online).
- [21] S. Page, Copper Deposits of The Tyrone District New Mexico, United States geological Survey, Department of the Interior, Professional paper 122, Washington, USA, Government printing Office 1922, pp 53.

TABLE 1: Chemical analyses of Thai cements (mass %)

Referanses	[7]	[8]	[9]	[10]	[9]	[11]	[12]	[13]	[14]
SiO <sub>2</sub>	21.16	19.5	20.8	20.62	21.85	20.73	20.8	18.74	16.37
Al <sub>2</sub> O <sub>3</sub>	5.09	5.84	5.5	5.22	5.39	4.7	5.2	5.22	3.85
Fe <sub>2</sub> O <sub>3</sub>	3.01	3.19	3.16	3.1	2.1	3.2	3.2	3.20	3.48
CaO	66.22	65.45	64.97	64.99	65.91	65.4	66.3	65.30	68.48
MgO	1.27	0.92	1.06	0.91	1.16	1.54	1.2	0.82	0.64
SO <sub>3</sub>	2.42	2.99	2.96	2.7	2.51	2.37	2.4	2.80	4.0
Na <sub>2</sub> O	0.04	0.07	0.08	0.07	NA	Na	0.1	0.08	0.06
K <sub>2</sub> O	0.25	0.63	0.55	0.5	0.31	Na	0.2	0.50	0.52
LOI	0.98		2.89	Na	0.96	1.34	Na	2.75	1.70

TABLE 2: EDX area analyses of sericite rock from sample 30-XA (mass %)

Component	NaO	MgO	Al <sub>2</sub> O <sub>3</sub>	SiO <sub>2</sub>	K <sub>2</sub> O	TiO <sub>2</sub>	MnO <sub>2</sub>	Fe <sub>2</sub> O <sub>3</sub>	Total
	0.37	1.56	26.2	62.05	5.76	0.61	Na	3.45	99.26
	0.37	1.16	26.38	63.09	5.79	0.59	Na	2.62	100
	0.43	2.22	34.29	53.38	7.29	0.86	Na	1.52	100
	0.37	2.3	34.63	53.1	7.62	0.6	Na	1.38	100
Average	0.39	1.81	30.38	57.91	6.62	0.67		2.24	99.82
<i>St. dev.</i>	<i>0.03</i>	<i>0.55</i>	<i>4.72</i>	<i>5.40</i>	<i>0.98</i>	<i>0.13</i>		<i>0.98</i>	<i>0.37</i>

TABLE 3: EDX area analysis of quartzite rock from sample 30-XB

Component	NaO	MgO	Al <sub>2</sub> O <sub>3</sub>	SiO <sub>2</sub>	K <sub>2</sub> O	TiO <sub>2</sub>	MnO <sub>2</sub>	Fe <sub>2</sub> O <sub>3</sub>	Total
	0.24	1.22	8.44	85.53	3.15	0.44	-	0.99	100

TABLE 4: Cracks in cement paste, cracks in coarse aggregates, crack index and reaction type

Parametre/sample	Cracks in cement paste (number/cm <sup>2</sup> )	Coarse with crack (%)	Coarse with crack out in cement paste (%)	Crack index	Reaction type*
30-XA	0.22	33.3	13.3	16.9	5
30-XB	0.15	45.7	14.3	14.7	5

\* Reaction type 5 when ASR cracks in the cement paste connect at least two reacted aggregates

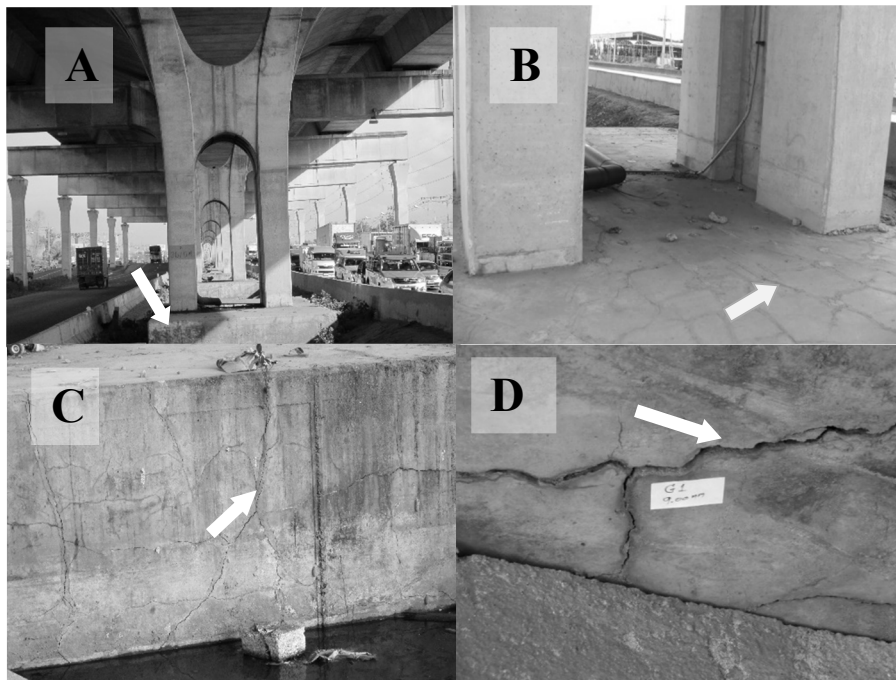


FIGURE 1: A: location of concrete foundations in the highway structure (arrow). B: foundation with repaired cracks (arrow). C and D: significant cracking with cracks up to 9 mm wide.

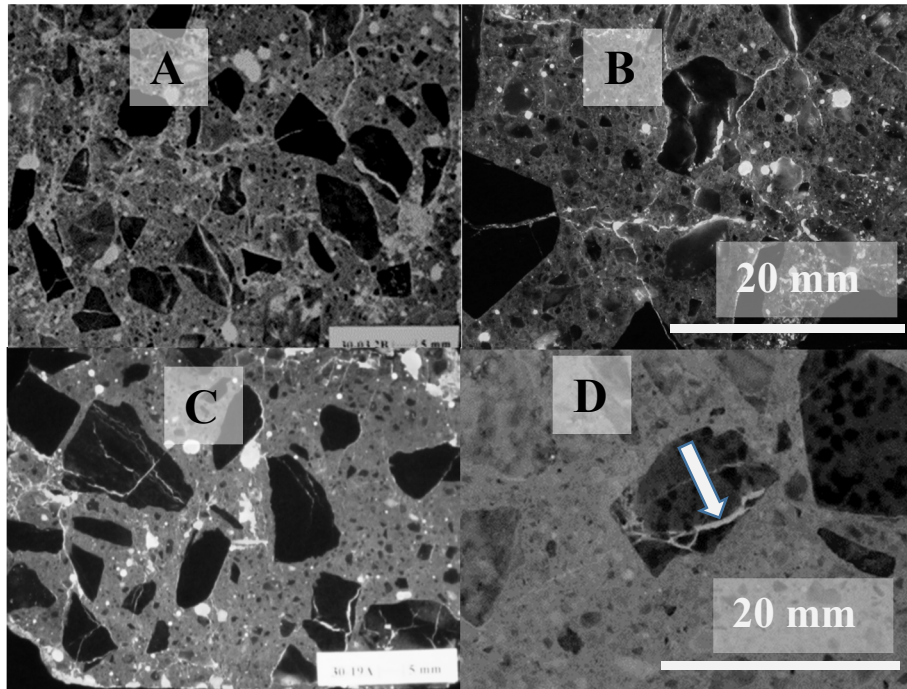


FIGURE 2 : A and B: (30-XB) cracks in aggregate (quartzite and granite) and cement paste. C: (30-XA): cracks in aggregate and cement paste (sericite rock). D: white reaction product (arrow) in intergranular crack in quartzite (30-XB). Photo A, B and C in fluorescence light.

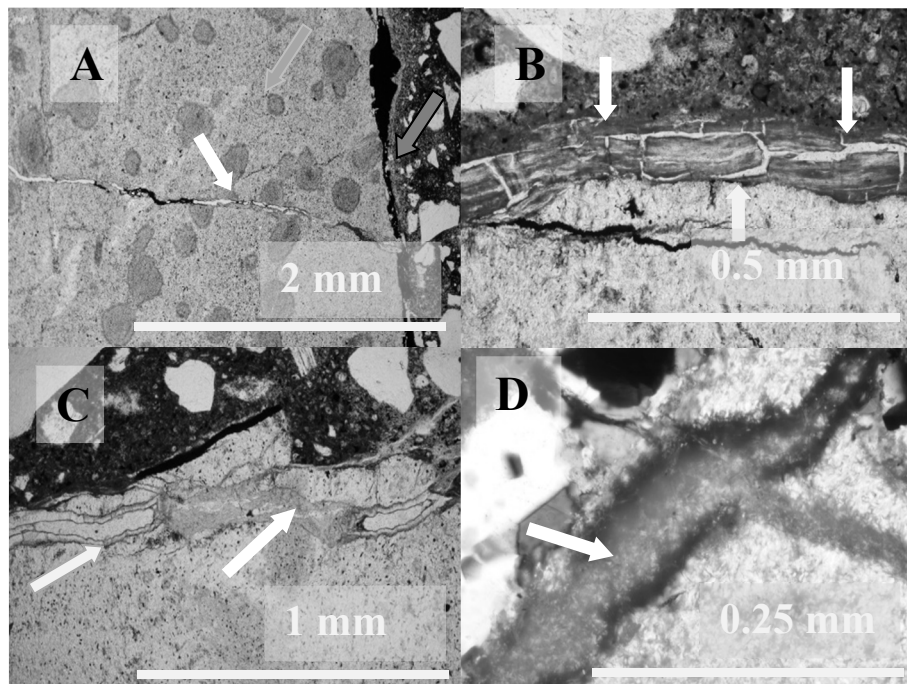


FIGURE 3: sample 30-XA photos of sericite rock: A: pseudomorph in sericite rock and cracks due to ASR (arrow). B: laminated amorphous gel in contact zone aggregate-cement paste. (arrow). C: gel and cryptocrystalline reaction product in sericite rock near interface to cement paste (arrow). D: cryptocrystalline reaction products in sericite rock, polarizing light (arrow).

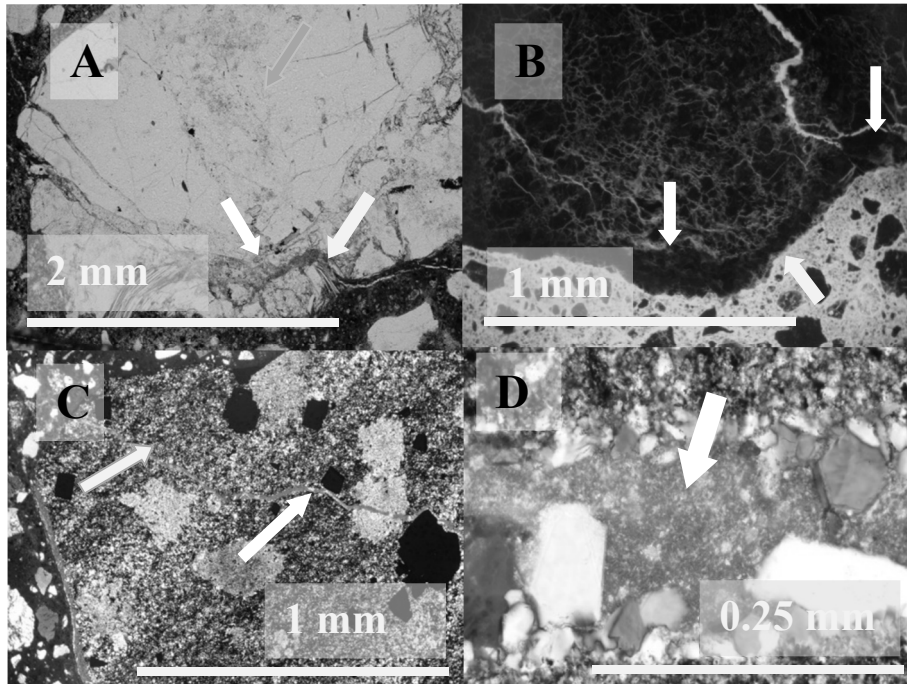


FIGURE 4 (sample 30-XB):A: reacted granite with cryptocrystalline reaction products in crack (arrows). B: reacted granite in fluorescence light. Note significant intergranular cracking and dense outer zone due to ASR (arrows). C: reacted quartzite in polarizing light. Note crack due to ASR (arrow) and pseudomorphs and opaque phases. D: quartzite in polarizing light; note cryptocrystalline reaction products in crack (arrow and salt and pepper texture) in cryptocrystalline reaction products.

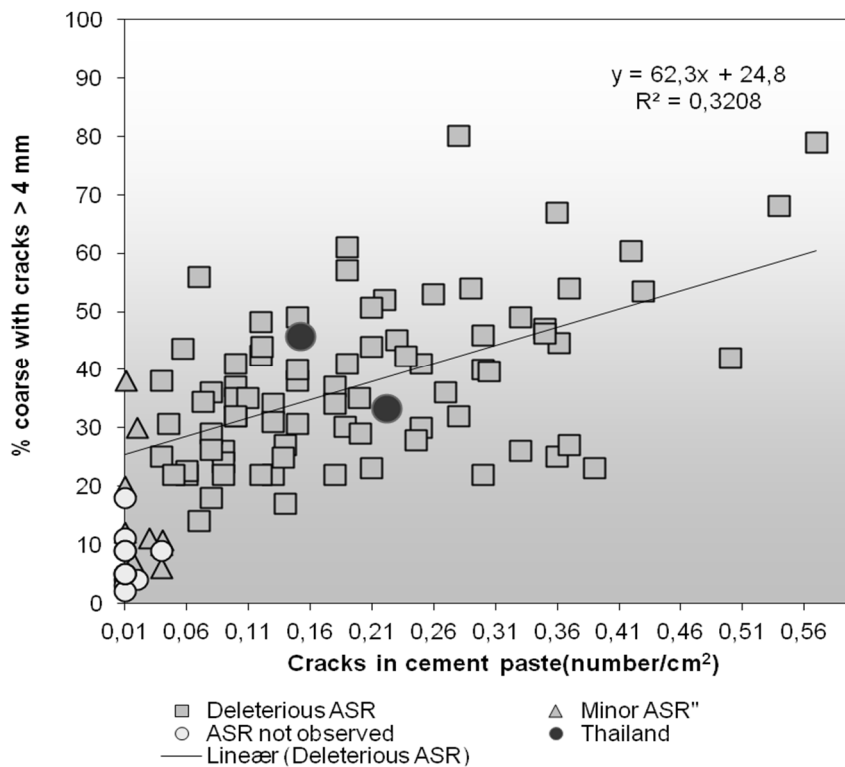


FIGURE 5: Plot of cracks in coarse aggregates versus cracks in cement paste, from sample 30-XA and 30-XB plotted together with Norwegian structures damaged by ASR